Coexistence of Jahn-Teller distortions in an O_h symmetry: A general view including the spin-orbit interaction

M. Bacci
Istituto di Ricerca sulle Onde Elettromagnetiche del Consiglio Nazionale delle Ricerche, Via Panciatichi 64, 50 127 Firenze, Italy

E. Mihóková and K. Polák
Institute of Physics, Czech Academy of Sciences, Cukrovarnická 10, 162 00 Prague 6, Czech Republic
(Received 20 January 1997)

The coexistence of distortions of different symmetry due to the quadratic Jahn-Teller interactions in an octahedral complex is revisited. Analytical expressions for the position and energy of the different stationary points are given; afterwards the influence of the spin-orbit coupling is numerically evaluated for the overall system ($^3T_1+{}^1T_1$), which is encountered in the excited configuration of ns^2 impurities. An evaluation of the magnitude of the Jahn-Teller effect for 6-, 8-, and 12-coordinated complexes is performed according to the angular overlap model. Particular attention is paid to parameter values consistent with the eight-coordinated CsX:Tl$^+$ systems (X=Cl, Br, I). The coexistence of trigonal minima with tetragonal or orthorhombic ones is found for a rather wide range of parameter values with the minima better pronounced in the singlet state ^1T even for high values of the spin-orbit coupling. [S0163-1829(97)00521-3]

I. INTRODUCTION

The static Jahn-Teller effect[1] (JTE) in a triply degenerate state T of an O_h complex interacting with vibrational modes of ϵ_g and τ_{2g} symmetry has been extensively studied for several years. A strong motivation has been to provide a theoretical explanation for the experimentally observed structure of absorption and emission bands of alkali halide phosphors doped with Tl$^+$-like impurity ions (see, e.g., the review articles in Refs. 2 and 3). The theoretical model based on the JT effect was introduced by Fukuda.[4]

In the case of linear JT coupling it has been shown[5] that tetragonal or trigonal stable distortions are possible according to the relative magnitude of the coupling constants b (ϵ_g modes) and c (τ_{2g} modes); moreover, orthorhombic stationary points exist on the lower-energy surface, but they are never minima. The extension up to second-order interactions[6,7] showed that orthorhombic points may become minima.

When the spin-orbit coupling is considered for the overall system ($^3T_{1u}+{}^1T_{1u}$), it was shown[8,9] that, if a strong difference in curvature is assumed between the ground and excited adiabatic potential energy surfaces (APES's), the JT coupling to ϵ_g modes only can produce two kinds of coexisting tetragonal minima on the Γ_4^- ($^3T_{1u}^*$) APES. In a more general theoretical investigation in the five-dimensional space of tetragonal and trigonal coordinates it was demonstrated[10,11] that not only can orthorhombic minima exist, but they can coexist with tetragonal ones for plausible values of the relevant parameters and for sufficiently low values of the spin-orbit (SO) coupling constant. Moreover, tetragonal minima can coexist with trigonal ones for similar values of the parameters. Further improvements were made by including the effect of anharmonicity[12] on the $T\otimes(\epsilon_g+\tau_{2g})$ JT problem. The performed analysis showed that the linear JTE together with anharmonicity may cause the orthorhombic points reported in Refs. 5 and 13 to become minima as well as allowing minima of different symmetry to coexist. Thus, the inclusion of anharmonicity leads to results analogous to those obtained with the quadratic JTE.

A rigorous analysis of the quadratic JTE terms, also involving the totally symmetrical vibrational mode Q_1, appeared in Ref. 14. It was limited to consideration of linear and bilinear terms containing Q_1 and the results confirmed the possibility of the coexistence of tetragonal and trigonal minima, while the orthorhombic points can never become minima in this framework. In Ref. 14 there was also made an estimate of JT coupling constants for real physical systems, namely, KCl:Tl$^+$, KBr:Tl$^+$, KI:Tl$^+$. Based on this estimate the coexistence of the different kinds of minima on APES's was then studied numerically. However, the role of the SO interaction, which has a non-negligible effect on the potential shape, especially in the case of Tl$^+$, was only glimpsed at.

From this discussion it can be seen that there is still no complete study of the APES's of the configuration containing both triplet $^3T_1$ and the singlet $^1T_1$ states in multidimensional space that includes all tetragonal and trigonal vibrational modes together with the spin-orbit interaction. (We henceforth drop the suffix u on $^3T_1$ and $^1T_1$ for simplicity.)

Moreover, recent experimental results on Tl$^+$ isolated centers built in CsCl, CsBr, and CsI crystals[15,16] with bcc crystal structure as well as those obtained for $KMgF_3$:Tl crystals[17] with perovskitelike structure would require an extension of the analysis to an 8 or 12 coordination around the central ion. In such an arrangement additional vibrational modes of ϵ_g and τ_{2g} symmetry occur. Nevertheless, a recent study of the $T\otimes(\epsilon+2\tau_2)$ JT problem for tetrahedral clusters[18] showed that the addition of an extra τ_{2g} mode does not introduce any extra minimum. A similar result is also valid for the $T\otimes(2\epsilon_g+2\tau_{2g})$ problem in 12-coordinated O_h complex so that the JT analysis in 8 and 12 coordination

can be easily reduced, *mutatis mutandis*, to the case of 6 coordination.

In the present work we report the results of a general study of the APES's in the excited states of luminescence centers for the overall problem $({}^3T_1+{}^1T_1)$ paying particular attention to the 8-coordinated arrangement, namely, for Cs-Cl:Tl, CsBr:Tl, and CsI:Tl, whose phenomenology has not been completely clarified yet. We considered both linear and quadratic JT terms that express coupling to the different modes of ϵ_g and τ_{2g} symmetry, together with spin-orbit interaction, by developing the analytical study as far as possible and then proceeding by numerical calculations.

II. GENERAL THEORY

A. Electron-lattice interaction

The Hamiltonian of the electron-lattice interaction can be written as[10]

$$\begin{aligned} H_{\rm el} &= W+V \\ &= \{-(3)^{-1/2}[2bQ_2+2b_{\epsilon\epsilon}Q_2Q_3+b_{\tau\tau}(Q_4^2-Q_5^2)] \\ &\quad\times\varepsilon_\epsilon-(3)^{-1/2}[2bQ_3+b_{\epsilon\epsilon}(Q_2^2-Q_3^2) \\ &\quad+(3)^{-1/2}b_{\tau\tau}(2Q_6^2-Q_4^2-Q_5^2)]\varepsilon_\Theta-(cQ_4+c_{\tau\tau}Q_5Q_6) \\ &\quad\times\tau_\xi-(cQ_5+c_{\tau\tau}Q_4Q_6)\tau_\eta-(cQ_6+c_{\tau\tau}Q_4Q_5)\tau_\zeta\} \\ &\quad+\{\tfrac{1}{2}[K_\epsilon(Q_2^2+Q_3^2)+K_\tau(Q_4^2+Q_5^2+Q_6^2)]\mathcal{I}\}, \end{aligned} \tag{1}$$

where Q_i are the symmetry coordinates transforming as ϵ_g (Q_2, Q_3) and τ_{2g} (Q_4, Q_5, Q_6); b, and c are the linear and electron-lattice coupling parameters; $b_{\epsilon\epsilon}$, $b_{\tau\tau}$, and $c_{\tau\tau}$ are the quadratic ones; ε_ϵ, ε_Θ, τ_ξ, τ_η, and τ_ζ are 3×3 matrices based on the orbital triplet functions $|x\rangle$, $|y\rangle$, and $|z\rangle$; $\mathcal{I}$ is the unit matrix; and K_ϵ and K_τ are the elastic constants for the ϵ_g and τ_{2g} modes, respectively. Here the $\epsilon_g\times\tau_{2g}$

TABLE I. Coordinates of stationary points in hexacoordinated geometry including quadratic JT effect. Only one distortion is considered; the others are obtained by applying symmetry rules.

Symmetry	D_{4h}	D_{3d}	$D_{2h}^{(1)}$	$D_{2h}^{(2)}$	$C_{2h}^{(1)}$	$C_{2h}^{(2)}$
Q_2	0	0	0	0	0	$\dfrac{b\left(K_\epsilon+\dfrac{2}{\sqrt{3}}b_{\epsilon\epsilon}\right)}{3(K_\epsilon^2-\frac{4}{9}b_{\epsilon\epsilon}^2)}$
Q_3	$\dfrac{-2b}{\sqrt{3}K_\epsilon-2b_{\epsilon\epsilon}}$	0	$\dfrac{b}{\sqrt{3}K_\epsilon+b_{\epsilon\epsilon}}$	$\dfrac{-5b}{4\sqrt{3}K_\epsilon-5b_{\epsilon\epsilon}}$	$\dfrac{-b}{\sqrt{3}K_\epsilon-b_{\epsilon\epsilon}}$	$\dfrac{b\left(K_\epsilon-\dfrac{2}{3\sqrt{3}}b_{\epsilon\epsilon}\right)}{\sqrt{3}(K_\epsilon^2-\frac{4}{9}b_{\epsilon\epsilon}^2)}$
Q_4	0	$\dfrac{-2c}{3K_\tau+4c_{\tau\tau}}$	0	$\overline{Q^0}$ [a]	$Q_T(C_{2h})$ [b]	0
Q_5	0	$\dfrac{-2c}{3K_\tau+4c_{\tau\tau}}$	0	$\overline{Q^0}$ [a]	$Q_T(C_{2h})$ [b]	0
Q_6	0	$\dfrac{-2c}{3K_\tau+4c_{\tau\tau}}$	$\dfrac{3c}{3K_\tau-2b_{\tau\tau}}$	$\overline{Q_T^0}$ [c]	$\dfrac{1}{\sqrt{6}}Q_T(C_{2h})$ [b]	$\dfrac{-2\sqrt{2}c}{3K_\tau-2b_{\tau\tau}}$
$E^{(0)}$	$\dfrac{-2b^2}{3K_\epsilon-2\sqrt{3}b_{\epsilon\epsilon}}$	$\dfrac{-2c^2}{3K_\tau+4c_{\tau\tau}}$	$E_{D1}^{(0)}$ [d]	$E_{D2}^{(0)}$ [e]	—	—
EQD[f]	3	4	6	6	12	12
PM[g]	y	y	y [h]	y [h]	n	n

[a] $\overline{Q^0}=\dfrac{(\sqrt{6}/4)c[-K_\tau-\frac{5}{6}b_{\tau\tau}+\frac{1}{4}c_{\tau\tau}]}{(\frac{1}{4}c_{\tau\tau}-\frac{5}{12}b_{\tau\tau}+K_\tau)(\frac{5}{6}b_{\tau\tau}+K_\tau)-\frac{3}{4}c_{\tau\tau}^2}$.

[b] $Q_T(C_{2h})=-\dfrac{\frac{2}{3}c(\frac{2}{3}b_{\tau\tau}+K_\tau-\frac{1}{3}c_{\tau\tau})}{(\frac{2}{3}b_{\tau\tau}+K_\tau)(-\frac{1}{3}b_{\tau\tau}+K_\tau+\frac{1}{3}c_{\tau\tau})-\frac{8}{9}c_{\tau\tau}^2}$.

[c] $\overline{Q_T^0}=\dfrac{(c/4)[-K_\tau+\frac{5}{12}b_{\tau\tau}+\frac{11}{4}c_{\tau\tau}]}{(\frac{1}{4}c_{\tau\tau}-\frac{5}{12}b_{\tau\tau}+K_\tau)(\frac{5}{6}b_{\tau\tau}+K_\tau)-\frac{3}{4}c_{\tau\tau}^2}$.

[d] $E_{D1}^{(0)}=\dfrac{-b^2}{2\sqrt{3}(\sqrt{3}K_\epsilon+b_{\epsilon\epsilon})}-\dfrac{3c^2}{2(3K_\tau-2b_{\tau\tau})}$.

[e] $E_{D2}^{(0)}=\dfrac{-25b^2}{8\sqrt{3}(4\sqrt{3}K_\epsilon-5b_{\epsilon\epsilon})}+\dfrac{c}{2}(\sqrt{6}\overline{Q^0}+\overline{Q_T^0})+\dfrac{\sqrt{6}}{2}c_{\tau\tau}\overline{Q^0}\,\overline{Q_T^0})+(K_\tau-\frac{5}{12}b_{\tau\tau}+\frac{1}{4}c_{\tau\tau})(\overline{Q^0})^2+(\frac{1}{2}K_\tau+\frac{5}{12}b_{\tau\tau})(\overline{Q_T^0})^2$.

[f] EQD: number of equivalent distortions for each set.

[g] PM: possibility of becoming minima.

[h] At the second order only.

TABLE II. Linear Jahn-Teller coupling constants according to AOM.

Coupling constant	6-coordinated	8-coordinated	12-coordinated
b	—	$\frac{4\sqrt{3}}{3R}(e_\sigma - e_\pi)$	$-\frac{\sqrt{6}}{R}(e_\sigma - e_\pi)$
b'	$\frac{\partial e_\sigma}{\partial R} - \frac{\partial e_\pi}{\partial R}$	—	$-\frac{1}{\sqrt{2}}\left(\frac{\partial e_\sigma}{\partial R} - \frac{\partial e_\pi}{\partial R}\right)$
c	—	$\frac{2\sqrt{2}}{3}\left(\frac{\partial e_\sigma}{\partial R} - \frac{\partial e_\pi}{\partial R}\right)$	$\left(\frac{\partial e_\sigma}{\partial R} - \frac{\partial e_\pi}{\partial R}\right)$
c'	$\frac{2}{R}(e_\sigma - e_\pi)$	$\frac{4}{3R}(e_\sigma - e_\pi)$	$-\frac{2}{R}(e_\sigma - e_\pi)$

terms are omitted as they do not change the results qualitatively and their effect has been discussed in Ref. 7.

Following the Öpik-Pryce procedure[5] we express the orbital electronic state as $a_1|x\rangle + a_2|y\rangle + a_3|z\rangle$. Then $H_{\rm el}$ operates on the column matrix a whose components are a_1, a_2, and a_3 and the coordinates Q_i^0 and the eigenvalues E_i^0 of the stationary points are given by the solutions of the system

$$\overline{a}\frac{\partial W}{\partial Q_i}a + \frac{\partial V}{\partial Q_i} = 0 \quad (i = 2, \ldots, 9),$$

$$H_{\rm el}a = Ea, \tag{2}$$

$$\sum_{k=1}^{3} a_k^2 = 1 \quad \text{where} \quad \overline{a}a = 1.$$

The results of the calculations are summarized in Table I. Some of the stationary points and energies have already been mentioned in Ref. 10, but we report them here for the sake of completeness. All the final symmetries given in Table I are in accordance with the procedure described in Ref. 19, using the concepts of kernels and epikernels.[20–22] Applying that procedure one can derive which symmetries are accessible by activating specific JT-active vibrational mode.

Equation (1) is valid for 6-coordinated octahedral complexes, but it can be easily extended to both 8 and 12 coordination by adding further symmetry coordinates τ_{2g} (8 coordination) and $\tau_{2g} + \epsilon_g$ (12 coordination). For example, if Q_4, Q_5, and Q_6 are three components for the stretching τ_{2g}^s mode in an 8-coordinated complex, the additional components of the bending τ_{2g}^b mode (Q_7, Q_8, Q_9) enter the Hamiltonian in terms analogous to those of Q_4, Q_5, and Q_6, only with the different coupling constants. These new coupling constants will be indicated by a prime (c', $c'_{\tau\tau}$, etc.) in the following. Furthermore, the relationships reported in Table I remain still valid, if the force and coupling constants are related to ''effective'' normal coordinates that are the linear combination of the original symmetry coordinates.

B. Full Hamiltonian

In order to obtain the equations of the potential energy surfaces relative to the states of the sp(a_{1g} t_{1u}) electronic configuration one has to diagonalize a 12×12 matrix

$$H = H_0 + H_{\rm el} + \zeta(\vec{l}_1\cdot\vec{s}_1 + \vec{l}_2\cdot\vec{s}_2), \tag{3}$$

referred to the basis functions of H_0 (which includes the exchange energy G):

$$^1T_1: \quad |X_+S_0\rangle, \quad |Y_+S_0\rangle, \quad |Z_+S_0\rangle,$$

$$^3T_1: \quad |X_-S_i\rangle, \quad |Y_-S_i\rangle, \quad |Z_-S_i\rangle, \quad i = x,y,z. \tag{4}$$

In the above equation, $X_\pm$, $Y_\pm$, and $Z_\pm$ are the symmetrized and antisymmetrized orbital functions given by

$$X_\pm = (1/\sqrt{2})\{a_{1g}(1)t_{1u}(2) \pm t_{1u}(1)a_{1g}(2)\}, \quad \text{etc.},$$

and S_x, S_y, S_z, and S_0 are triplet and singlet spin functions given by

$$S_x = -(1/\sqrt{2})\{\alpha(1)\alpha(2) - \beta(1)\beta(2)\},$$

$$S_y = (i/\sqrt{2})\{\alpha(1)\alpha(2) + \beta(1)\beta(2)\},$$

$$S_z = (1/\sqrt{2})\{\alpha(1)\beta(2) + \beta(1)\alpha(2)\},$$

$$S_0 = (1/\sqrt{2})\{\alpha(1)\beta(2) - \beta(1)\alpha(2)\}.$$

The full Hamiltonian matrix written in this basis is

$$H=\begin{pmatrix}
 & & & 0 & -1 & 0 & 0 & 0 & -1 & 0 & 0 & 0 \\
 & H_{\rm el}^3 & & 1 & 0 & 0 & 0 & 0 & 0 & 0 & 0 & -i \\
 & & & 0 & 0 & 0 & 1 & 0 & 0 & 0 & i & 0 \\
0 & 1 & 0 & & & & 0 & 0 & 0 & 0 & 0 & i \\
-1 & 0 & 0 & & H_{\rm el}^3 & & 0 & 0 & -1 & 0 & 0 & 0 \\
0 & 0 & 0 & & & & 0 & 1 & 0 & -i & 0 & 0 \\
0 & 0 & 1 & 0 & 0 & 0 & & & & 0 & -i & 0 \\
0 & 0 & 0 & 0 & 0 & 1 & & H_{\rm el}^3 & & i & 0 & 0 \\
-1 & 0 & 0 & 0 & -1 & 0 & & & & 0 & 0 & 0 \\
0 & 0 & 0 & 0 & 0 & i & 0 & -i & 0 & & & \\
0 & 0 & -i & 0 & 0 & 0 & i & 0 & 0 & & H_{\rm el}^1 & \\
0 & i & 0 & -i & 0 & 0 & 0 & 0 & 0 & & &
\end{pmatrix}, \tag{5}$$

where $H_{\rm el}^3=H_{\rm el}+E_0(^3T_1)\times\mathcal{I}$ and $H_{\rm el}^1=H_{\rm el}+E_0(^1T_1)\times\mathcal{I}$; $H_{\rm el}$ is given by Eq. (1) [except that the ε_ϵ, ε_Θ, τ_ξ, τ_η, and τ_ζ are now 3×3 matrices based on the functions (4)]; $\mathcal{I}$ is the 3×3 unit matrix, $E_0(^3T_1)=W_0-G$, and $E_0(^1T_1)=W_0+G$ are the energies of the orbital triplet and singlet states, respectively, and G is the energy of the exchange interaction.

III. APPLICATION TO Cs-HALIDE SYSTEMS

In this section we perform the diagonalization of the full Hamiltonian (5) for the systems CsX:Tl$^+$ (X=Cl, Br, I). This analysis will also use the results summarized in Table I.

First we perform an estimate of the linear coupling parameters to ϵ_g and τ_{2g} modes using the angular overlap model. We also estimate the force constants. We then study the APES's and the possibility of the coexistence of the minima of different symmetry. We do this by varying the parameters of the quadratic JT coupling and of the SO coupling.

A. Evaluation of linear Jahn-Teller coupling constants and force constants

Linear Jahn-Teller coupling constants were derived using a method based on the angular-overlap model (AOM),[23,19] that is, a simplified molecular-orbital linear-combination-of-atomic-orbitals (MO-LCAO) method.[24] In this framework one can obtain the relationships valid for ns^2 impurities in the 6-, 8-, and 12-coordinated arrangements of neighboring atoms summarized in Table II. Here b, b', c, and c' are the linear coupling constants with tetragonal bending, tetragonal stretching, trigonal stretching, and trigonal bending modes, respectively. R is the metal ligand bond length, e_λ is the energy change of the impurity p orbital due to the interaction with a ligand orbital, and λ indicates the bonding symmetry (σ, π) with respect to the metal-ligand axis. In the angular overlap model e_λ is given by

$$e_\lambda=K_\lambda S_\lambda^2, \tag{6}$$

where S_λ is the diatomic overlap integral and K_λ a proportionality constant. In the Wolfsberg-Helmholz approximation[25] K_λ can be expressed as

$$K_\lambda\approx H_X^2/(H_M-H_X). \tag{7}$$

Here H_M and H_X are the diagonal matrix elements of the metal and ligand orbitals, respectively. If K_λ is assumed to be independent of the bond length, the first derivatives can be obtained as

$$\frac{\partial e_\lambda}{\partial R}\approx K_\lambda\frac{\partial S_\lambda^2}{\partial R}. \tag{8}$$

On this basis we have attempted to estimate the linear coupling constants for the 8-coordinated O_h systems CsX:Tl$^+$ (X=Cl, Br, I). Since we were interested only in an approximate evaluation of the parameters, we limited ourselves to a molecular-orbital analysis based on extended Hückel calculations. In evaluating the parameter K_λ the values for H_X and H_M corresponding to the valence-orbital ionization energies of the free atoms have been used. It could be argued that the values for a free ion would be more appropriate for the systems considered. On the other hand, free ion values can result in overestimation K_λ in cases where the difference H_M-H_X is rather small, as pointed out in Ref. 14. The diatomic overlap integrals have been computed for a Tl-X distance corresponding to the crystals under consideration using Slater-type orbitals. In this way the values of e_σ and e_π have been obtained from Eq. (6). For the evaluation of the first derivatives $\partial e_\lambda/\partial R$, it is necessary to have the first derivative $\partial S_\lambda^2/\partial R$. This can be obtained by realizing[23] that in a small range of bond distances the overlap integral S_λ is a nearly linear function of R:

$$S_\lambda\approx a_\lambda+b_\lambda R. \tag{9}$$

It easily follows from this that

$$S_\lambda^2=A_\lambda R^2+B_\lambda R+C_\lambda \tag{10}$$

and

TABLE III. Parameter values of Cs-halide systems.

System	b [eV/Å]	c' [eV/Å]	c [eV/Å]	K_ϵ [eV/Å^2]	K_τ [eV/Å^2]	K'_τ [eV/Å^2]	2Δ [eV]
CsCl:Tl$^+$	0.7	0.4	−1.24	2	2	2	1.32
CsBr:Tl$^+$	0.55	0.32	−1.31	1	1	1	1.08
CsI:Tl$^+$	0.44	0.25	−1.16	0.7	0.7	0.7	0.99

$$\frac{\partial S_\lambda^2}{\partial R} = 2A_\lambda R + B_\lambda . \tag{11}$$

Computing the dependence $S_\lambda^2 = S_\lambda^2(R)$ and fitting it by the function (10), we obtained the parameters A_λ and B_λ for evaluating $\partial S_\lambda^2/\partial R$ and $\partial e_\lambda/\partial R$ as well. All these results are summarized in Table III.

In the evaluation of the force constants the following procedure was used. The complex TlX_8 was subjected to deformation according to the desired symmetry as if interacting with JT coordinates of tetragonal or trigonal symmetry. For a succession of deformations, the total energy of the deformed complex was computed. This provided energy as a function of the deformation coordinate. Assuming that near the bottom of the well this dependence can be expressed in the form

$$E = E_0 + \tfrac{1}{2}K(Q - Q_0)^2, \tag{12}$$

where E_0 is the energy of the minimum at Q_0, the force constant K was then extracted from the fitting procedure.

IV. RESULTS OF NUMERICAL ANALYSIS AND DISCUSSION

For the cases of CsCl:Tl and CsI:Tl, the coexistence of minima of different symmetry was studied for a wide range of parameter values for quadratic JT coupling. We also checked the general conditions for coexistence reported in Ref. 10. As the value of the trigonal stretching coupling constant c is substantially higher than that of c' for trigonal bending (see Table III), the quadratic coupling constants $c'_{\tau\tau}$ and $b'_{\tau\tau}$ were set to zero in order to reduce the number of free parameters entering the calculation. In the case of CsCl:Tl, without considering SO coupling, the coexistence of minima of different symmetry was found for the intervals given in Table IV.

For the systems under consideration, $c > b$, so that according to Ref. 5 without taking into account the quadratic Jahn-Teller coupling the linear JT parameters favor the existence of trigonal minima under the assumption of similar force constants for the two vibrational modes. Different values of quadratic JT parameters enable the coexistence of the trigonal minima with minima of different symmetry. The value of parameter $b_{\epsilon\epsilon}$ plays a particularly important role relative to the value of b. Values of $b_{\epsilon\epsilon}$ less than b (including negative values) favor the coexistence with the orthorhombic minima, while $b_{\epsilon\epsilon} > b$ (>0) favors coexistence with tetragonal minima.

TABLE IV. Range of coexistence of minima of different symmetry on APES's in Cs-halide systems (quadratic JT coupling constants in eV/Å^2); linear JT constants and elastic constants are those reported in Table III.

System	Trigonal+orthorhombic	Trigonal+tetragonal
CsCl:Tl$^+$	$-3.3 < b_{\epsilon\epsilon} \leq 1$	$0.7 < b_{\epsilon\epsilon} < 1.7$
	$-1 \leq b_{\tau\tau} < 3$	$-1.3 \leq b_{\tau\tau} \leq 2.6$
	$-0.6 \leq c_{\tau\tau} < 1.2$	$-1 \leq c_{\tau\tau} < 1.2$
CsI:Tl$^+$	$-1.1 < b_{\epsilon\epsilon} \leq 0.45$	$0.3 < b_{\epsilon\epsilon} < 0.5$
	$-0.3 \leq b_{\tau\tau} < 0.6$	$-1 < b_{\tau\tau} \leq 0.3$
	$-0.2 \leq c_{\tau\tau} < 1$	$-0.3 \leq c_{\tau\tau} \leq 1$

It is of interest that for a limited range of values of $b_{\epsilon\epsilon} \approx b$, the coexistence of all three kinds of minima was found, as visualized in the energy map of Fig. 1. All points were checked to be true minima. Nevertheless, as will be pointed out later this coexistence is possible only for weak spin-orbit coupling.

When the SO coupling is introduced, one has to consider the interweaving of the roles of ζ (SO coupling constant) and G (exchange energy), resulting from the relationships[2]

$$E(^3T_1) = \Delta_1^3 = F_0 - \tfrac{1}{4}\zeta - \sqrt{(G+\tfrac{1}{4})^2 + \tfrac{1}{2}\lambda^2\zeta^2}, \tag{13}$$

$$E(^1T_1) = \Delta_1^1 = F_0 - \tfrac{1}{4}\zeta + \sqrt{(G+\tfrac{1}{4})^2 + \tfrac{1}{2}\lambda^2\zeta^2}. \tag{14}$$

From this it follows that the energy distance between $^3T_1$ and $^1T_1$ states is

$$|\Delta_1^3 - \Delta_1^1| = 2\sqrt{(G+\tfrac{1}{4})^2 + \tfrac{1}{2}\lambda^2\zeta^2} = 2\Delta. \tag{15}$$

Using the fact that the value of the parameter $\lambda \approx 1$,[2] to a good approximation, one can find the relationship between G and ζ depending on the energy distance Δ:

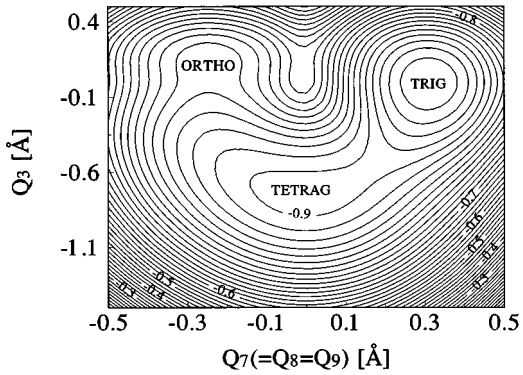

FIG. 1. Energy map in the $Q_3 - Q_7$ ($Q_7 = Q_8 = Q_9$, $Q_2 = 0$, $Q_4 = Q_5 = Q_6 = -0.13$ Å) space of Γ_4^- APES for CsCl:Tl$^+$ showing a trigonal minimum (TRIG), tetragonal minimum (TETRAG), and projection of the orthorhombic minima (ORTHO). Values of parameters used in the calculation are $b_{\epsilon\epsilon} = 0.8$ eV/Å^2, $b_{\tau\tau} = 0.3$ eV/Å^2, $c_{\tau\tau} = 0.5$ eV/Å^2, $\zeta = 0.1$ eV, and $G = 0.63$ eV. (Labels of contour lines are in eV.)

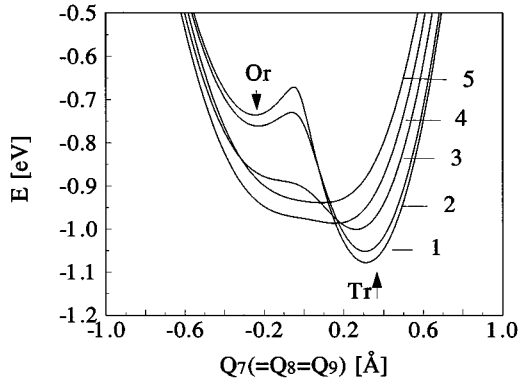

FIG. 2. Coexistence of a trigonal Tr minima and (a projection of) an orthorhombic Or minima on the Γ_4^- APES for CsCl:Tl^+. Effect of SO coupling (cross section along the Q_7 axis; $Q_7=Q_8=Q_9$, $Q_2=Q_3=0$, $Q_4=Q_5=Q_6=Q^0$). Values used in the calculation are $b_{\epsilon\epsilon}=-1.5$ eV/Å^2, $b_{\tau\tau}=0.3$ eV/Å^2, and $c_{\tau\tau}=0.5$ eV/Å^2. The values of ζ and G are varied. In curve 1, $\zeta=0.1$ eV, $G=0.63$ eV ($Q^0=-0.13$ Å); in curve 2, $\zeta=0.2$ eV, $G=0.59$ eV ($Q^0=-0.13$ Å); in curve 3, $\zeta=0.5$ eV, $G=0.43$ eV ($Q^0=-0.1$ Å); in curve 4, $\zeta=0.7$ eV, $G=0.28$ eV ($Q^0=-0.04$ Å); in curve 5, $\zeta=0.8$ eV, $G=0.14$ eV ($Q^0=-0.04$ Å).

$$G\approx-\frac{\zeta}{4}+\sqrt{\Delta^2-\frac{\zeta^2}{2}}. \tag{16}$$

Since to a good approximation 2Δ can be assumed equal to the energy distance between A and C absorption bands reported from the experimental observation (see Table III), we have investigated a set of values for ζ and G satisfying Eq. (16).

In the range of JT quadratic coupling constants, where the coexistence of trigonal and orthorhombic minima is allowed, a higher value of ζ diminishes the depths of the minima and shifts their position towards the undistorted position. For negative values of the parameter $c_{\tau\tau}$, the trigonal minima are more pronounced; the same is true for high values of ζ. Raising the parameter $c_{\tau\tau}$, the minima become less pronounced (see Fig. 2). Nevertheless, for the highest value of ζ, they are still present. Actually, for the crystal CsCl:Tl, the high values $\zeta\approx0.7-0.8$ are expected (according to the values of ζ and G reported in Ref. 17 for KX:Tl (X=Cl, Br, I) crystals, i.e., crystals whose distances between the A and C bands are similar to those of CsX:Tl).

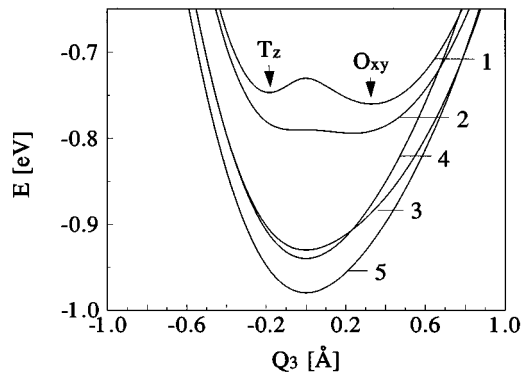

FIG. 3. The same as Fig. 2, but showing the orthorhombic minimum on the Γ_4^- APES; the cross section is along the Q_3 axis (the other $Q_i=0$).

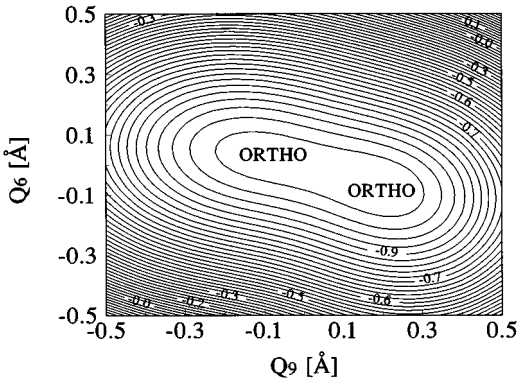

FIG. 4. Energy map in the Q_6-Q_9 space (the other $Q_i=0$) of the Γ_4^- APES for CsCl:Tl^+ showing existence of orthorhombic minima at the high value of ζ ($\zeta=0.7$ eV, $G=0.28$ eV); this corresponds to Fig. 3, curve 5. (Labels of contour lines are in eV.)

The situation for orthorhombic minima is presented in Fig. 3. With increasing ζ the component Q_3 of the orthorhombic stationary points vanishes; nevertheless, the minima are still present (see Fig. 4). These minima correspond to zero deformation along the Q_3 axis, but their symmetry remains unchanged (D_{2h}).

In the small range of parameters where the coexistence of all three kinds of minima becomes possible, ζ has a significant influence on tetragonal and orthorhombic minima; see Fig. 5. Starting from intermediate values of ζ the tetragonal minima vanish. In fact they coalesce with the orthorhombic minima. Those minima correspond to the minima with zero deformation along the Q_3 axis—in the same way as mentioned above. This is opposite to the coalescence of the orthorhombic minima into tetragonal ones for some kind of parameters, as pointed out in Ref. 10. Nevertheless, in our case this means that even if the values of the JT coupling constants for the system considered would favor the coexistence of all three kinds of minima of different symmetry, the high value of SO coupling would make such a coexistence impossible.

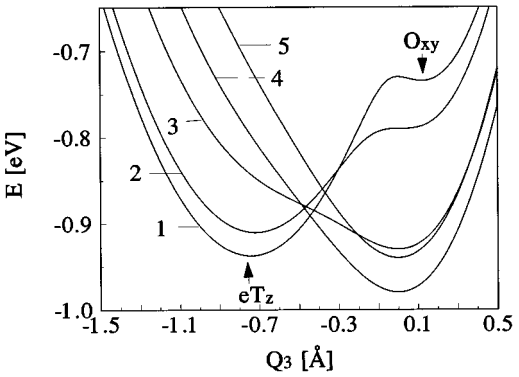

FIG. 5. Coexistence of tetragonal, trigonal, and orthorhombic minima (the same as Fig. 1): cross section along the Q_3 axis (the other $Q_i=0$) showing the effect of SO coupling on tetragonal (eTz) and orthorhombic (O_{xy}) minima. In curve 1, $\zeta=0.1$ eV, $G=0.63$ eV; in curve 2, $\zeta=0.2$ eV, $G=0.59$ eV; in curve 3, $\zeta=0.5$ eV, $G=0.43$ eV; in curve 4, $\zeta=0.7$ eV, $G=0.28$ eV; in curve 5, $\zeta=0.8$ eV, $G=0.14$ eV.

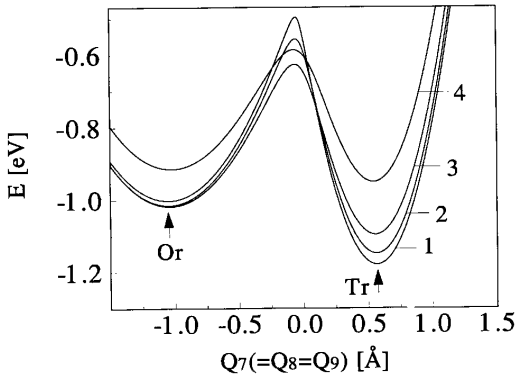

FIG. 6. Coexistence of trigonal and orthorhombic minima on the Γ_4^- APES showing the trigonal minimum (Tr) and projection of orthorhombic minima (Or), for CsI:Tl^+. Effect of SO coupling (cross section along the Q_7 axis; $Q_7=Q_8=Q_9$, $Q_2=Q_3=0$, $Q_4=Q_5=Q_6=-0.25$ Å). Values used in the calculation are $b_{\epsilon\epsilon}=-0.1$ eV/Å^2, $b_{\tau\tau}=0.2$ eV/Å^2, and $c_{\tau\tau}=0.5$ eV/Å^2; in curve 1, $\zeta=0.1$ eV, $G=0.46$ eV; in curve 2, $\zeta=0.2$ eV, $G=0.42$ eV; in curve 3, $\zeta=0.5$ eV, $G=0.34$ eV; in curve 4, $\zeta=0.7$ eV, $G=0.15$ eV.

Raising the parameter $b_{\epsilon\epsilon}$, only the coexistence of tetragonal minima with trigonal ones becomes possible and tetragonal minima are significantly pronounced also for high values of ζ. However, again a lower depth of minima corresponds to the higher ζ.

For the case of CsI:Tl the range of coexistence without consideration of SO coupling is also shown in Table IV. For this system a lower value of the SO coupling constant is expected relative to CsCl:Tl, namely, $\zeta\approx 0.4-0.5$ [considering the value reported for KI:Tl (Ref. 17)]. Also this lower value of ζ has less affect on the APES's compared to the previous case, as shown, e.g., in Fig. 6. With increasing ζ, the depth of the minima is lowered but the position of the minima remains almost unchanged. The most affected are orthorhombic minima where, similar to CsCl:Tl, the deformation along the Q_3 axis vanishes with higher ζ.

Coexistence of tetragonal minima with trigonal ones was found for a rather small range of parameter values, but as some uncertainty in the determination of linear coupling constants could also be expected, a slight change of these values would cause the coexistence to become more possible. On the other hand, the coexistence of tetragonal minima with orthorhombic ones is even more limited; as in the previous case it occurs only for values of the parameter $b_{\epsilon\epsilon}\approx b$. An example of such a coexistence is shown in Figs. 7(a) and 7(b).

Detailed calculations for the system CsBr:Tl were not performed, as from Table III it could be seen that all the parameter values are intermediate between those of CsCl and CsI. (The only exception is the parameter c, but as pointed out in Ref. 23 the stretching parameters are less accurate than those of bending.)

All the calculations were performed by diagonalizing the full 12×12 matrix and examples of the cross sections of all APES's are given in Figs. 8 and 9. For low values of the SO coupling the minimum for a singlet state APES has practically the same position as in the triplet state. For high values of SO coupling the depth of the minima is lowered and they

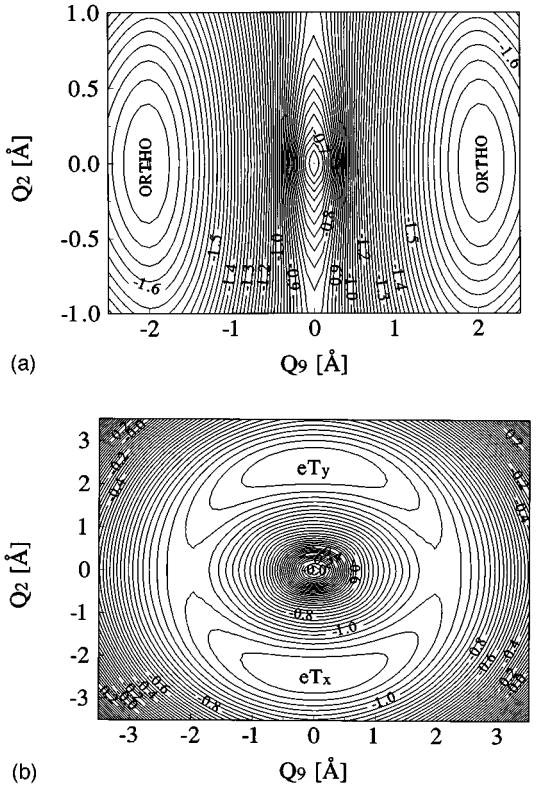

FIG. 7. (a) Energy map in Q_2-Q_9 space of the Γ_4^- APES for CsI:Tl^+ showing the coexistence of orthorhombic and tetragonal minima (Fig. 6). Here two orthorhombic minima are shown; for the left half-plane $Q_6=0.36$ Å, for the right half-plane $Q_6=-0.36$ Å; $Q_3=0.26$ Å ($Q_4=Q_5=Q_7=Q_8=0$). Values used in the calculation are $b_{\epsilon\epsilon}=0.45$ eV/Å^2, $b_{\tau\tau}=0.2$ eV/Å^2, $c_{\tau\tau}=0.5$ eV/Å^2, and $\zeta=0$. (b) The same as (a), except that $Q_3=1.4$ Å and the other $Q_i=0$, showing two tetragonal minima eT_x and eT_y on the Γ_4^- APES. (Labels of contour lines are in eV.)

are also shifted towards the undistorted state, but the shift of the minima in particular cases is more significant than that in a triplet state. On the other hand, as can be seen from Fig. 8 for the case of parameter values where the tetragonal mini-

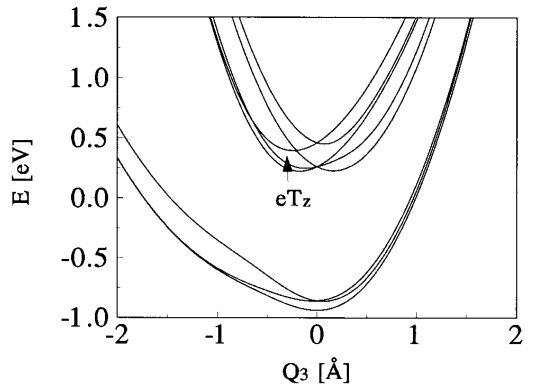

FIG. 8. Cross section along the Q_3 axis of all APES's on the $^3T_1$ and the $^1T_1$ levels of CsCl:Tl^+. The arrow shows the tetragonal minimum on the APES in the singlet state while the minimum on the lowest triplet state is no longer present. Values used in the calculation are $b_{\epsilon\epsilon}=0.8$ eV/Å^2, $b_{\tau\tau}=0.3$ eV/Å^2, $c_{\tau\tau}=0.5$ eV/Å^2, $\zeta=0.8$ eV, and $G=0.14$ eV.

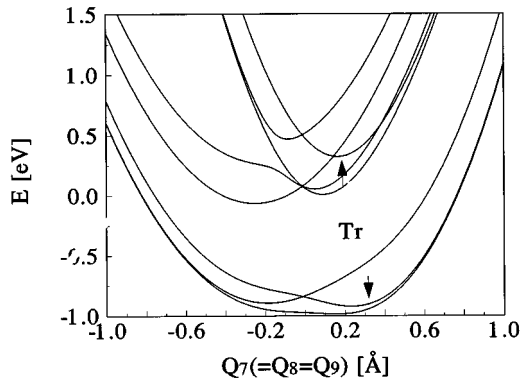

FIG. 9. Cross section along the Q_7 axis ($Q_7=Q_8=Q_9$; $Q_2=Q_3=0$, $Q_4=Q_5=Q_6=-0.04$ Å) of all APES's on the $^3T_1$ and the $^1T_1$ levels of CsCl:Tl$^+$ showing the trigonal minima in the lowest triplet and singlet states. Values used in the calculation are $b_{\epsilon\epsilon}=0.8$ eV/Å^2, $b_{\tau\tau}=0.3$ eV/Å^2, $c_{\tau\tau}=0.5$ eV/Å^2, $\zeta=0.8$ eV, and $G=0.14$ eV.

mum vanishes in the triplet state, it is still pronounced in the singlet state. The same feature was also found for the trigonal minima for the other systems where the tendency to ''wash out'' the minima by spin-orbit coupling can occur.

V. CONCLUSION

The results obtained in the present work show the possibility of coexisting minima of different symmetry on APES's of both singlet and triplet states. In particular cases the coexistence of three kinds of minima has been found (as already pointed out in Ref. 10), but because of a very limited range of JT coupling parameters, this possibility is rather improbable within the approach used. Moreover, the expected high value of the SO coupling constant (in actual cases) makes this coexistence impossible anyway.

Recent experimental results on the systems CsX:Tl (X=Cl, Br, I) (Refs. 15 and 16) showed the presence of two ultraviolet emission bands (under the excitation in the A absorption band). These were interpreted as emissions that occur from different kinds of minima coexisting on APES's of the triplet state of an impurity ion Tl$^+$, according to the analogy with fcc systems. Based on the polarization measurements of the emission, their symmetry was determined to be tetragonal and trigonal in the case of CsCl:Tl and CsBr:Tl. For CsI:Tl only the tetragonal symmetry of the A_T band was ascribed as a result of an experiment while the trigonal symmetry was ascribed to the other band, supposing the analogy with fcc systems. Our analysis does show the possibility of the coexistence of tetragonal and trigonal minima on the APES's of the triplet state; such a coexistence is more probable than the coexistence of tetragonal-orthorhombic minima. Thus to propose trigonal minima in the case of CsI:Tl, where experimental results are lacking, appears to be more plausible from our results as well.

Moreover, it has to be remarked that JT minima in the singlet state $^1T_1$ are less affected by the SO coupling and persist even when SO coupling has washed out the JT distortions in the triplet state. This fact could be of interest in interpreting absorption and emission features of these systems.

Finally we emphasize that, notwithstanding our interest in doped cesium-halide systems, the results presented could have more general application to the many physical systems where electronic T levels are found.

ACKNOWLEDGMENTS

One of the authors (E.M.) wishes to thank NATO for support. Support was also provided by AV CR Grant No. A1010505. Thanks are expressed to Dr. Carlo Mealli, ISSECC-CNR, Florence, who supplied us with a copy of the MOAN program.[26]

[1] H. A. Jahn and E. Teller, Proc. R. Soc. London, Ser. A **161,** 220 (1937).
[2] A. Ranfagni, D. Mugnai, M. Bacci, G. Viliani, and M. P. Fontana, Adv. Phys. **32**, 824 (1983).
[3] P. W. M. Jacobs, J. Phys. Chem. Solids **52**, 35 (1991).
[4] A. Fukuda, Phys. Rev. B **1**, 4161 (1970).
[5] U. Öpik and M. H. L. Pryce, Proc. R. Soc. London, Ser. A **238**, 425 (1957).
[6] S. Muramatsu and T. Iida, J. Phys. Chem. Solids **31**, 2209 (1970).
[7] I. B. Bersuker and V. Z. Polinger, Phys. Lett. **44A**, 495 (1973).
[8] A. Ranfagni and G. Viliani, Phys. Rev. B **9**, 4448 (1974).
[9] A. Ranfagni and G. Viliani, J. Phys. Chem. Solids **35**, 25 (1974).
[10] M. Bacci, A. Ranfagni, M. P. Fontana, and G. Viliani, Phys. Rev. B **11**, 3052 (1975).
[11] M. Bacci, M. P. Fontana, A. Ranfagni, and G. Viliani, Phys. Lett. **50A**, 405 (1975).
[12] M. Bacci, A. Ranfagni, M. Cetica, and G. Viliani, Phys. Rev. B **11**, 5907 (1975).
[13] P. Wysling and K. A. Müller, Phys. Rev. **173**, 327 (1968).
[14] A. Ranfagni, D. Mugnai, M. Bacci, M. Montagna, O. Pilla, and G. Viliani, Phys. Rev. B **20**, 5358 (1979).
[15] V. Nagirnyi, A. Stolovich, S. Zazubovich, V. Zepelin, E. Mihokova, M. Nikl, G. P. Pazzi, and L. Salvini, J. Phys. Condens. Matter **7**, 3637 (1995).
[16] E. Mihokova, V. Nagirnyi, M. Nikl, A. Stolovich, G. P. Pazzi, S. Zazubovich, and V. Zepelin, J. Phys. Condens. Matter **8**, 4301 (1996).
[17] A. Scacco, S. Fioravanti, M. Missori, U. M. Grassano, A. Lucci, M. Palummo, E. Giovenale, and N. Zema, J. Phys. Chem. Solids **54**, 1035 (1993).
[18] P. J. Kirk, C. A. Bates, and J. L. Dunn, J. Phys. Condens. Matter **6**, 5465 (1994).
[19] A. Ceulemans, D. Beyens, and L. G. Vanquickenborne, J. Am. Chem. Soc. **106**, 5824 (1984).
[20] M. A. Melvin, Rev. Mod. Phys. **28**, 18 (1956).
[21] E. J. Ascher, J. Phys. C **10**, 1365 (1977).
[22] P. Murray-Rust, H. B. Bürgi, and J. D. Dunitz, Acta Crystallogr. Sec. A **35**, 703 (1979).
[23] M. Bacci, Chem. Phys. **40**, 237 (1979).
[24] C. E. Schäffer and C. K. Jorgensen, Mol. Phys. **9**, 401 (1965).
[25] M. Wolfsberg and L. Helmholz, J. Chem. Phys. **20**, 837 (1952).
[26] C. Mealli and D. M. Proserpio, J. Chem. Educ. **67,** 399 (1990).